Paper IV

Oxidation of Cr(II) to Cr(III) on Reduced Cr/silica, with Implications for Catalytic Dehydrogenation of Ethane

Sindre Lillehaug[a] and Knut J. Børve[a]

(Dated: May 1, 2006)

The oxidation of chromium from oxidation state +II to +III on the surface of amorphous silica with water as oxidizing agent has been investigated by means of cluster models and density functional theory. It appears that hydrolysis of Cr(II)–OSi bonding leaves mononuclear chromium(II) mobile on the silica surface. Cr(II) gains mobility by moving from one silicon tetrahedron to the next through a series of synchromized formation and breaking of Cr–O and Si–O bonds. Oxidation to chromium(III) takes place in the encounter between two Cr(II)OH moieties. In the presence of moisture, the product is found to be a μ-oxo-bis[hydroxochromium(III)] species. These result have implications regarding the structure of Cr(III) species that are active in catalytic dehydrogenation of ethane. In particular, it appears that active Cr(III) can be an oligomer even if derived from mononuclear Cr(VI).

Keywords: Cr/silica,ethane,dehydrogenation,DFT,cluster,surface catalyst

I. INTRODUCTION

Chromium dispersed on various oxides exhibits catalytic properties with respect to dehydrogenation of short alkanes as well as for polymerization of ethylene. [1, 2] While this system has received continuous attention since 1933 when Cr/alumina was found to catalyze the dehydrogenation reaction, [3] due to the highly heterogeneous surface, most details regarding the nature of the active chromium species remain uncertain.

Chromium is usually anchored to the oxide support by calcination, i. e. by heating in oxygen. The chromium species formed are highly oxidized, and Cr(VI) is known to dominate strongly over Cr(V). [4] The active catalyst is obtained by reducing the sample, accompanied by removal of oxo ligands from chromium. [5, 6] The degree of reduction depends on the particular oxide support, chromium loading, choice of reducing agent, and conditions such as temperature and gas flow velocity. While alumina tends to stabilize chromium in oxidation state +III, [4, 7, 8] the Cr(II)/Cr(III) ratio on silica is more tunable. Reduction by carbon monoxide renders chromium mainly in oxidation state +II. [7, 9–12] H_2 or alkanes as reducing agents give a Cr(II)/Cr(III) ratio which decreases with increasing chromium loading. [13] Moreover, water is evolved during this reaction and appears to oxidize Cr(II) to Cr(III) unless evaporated. [9]

In the modern literature of catalytic dehydrogenation over Cr/oxide, most of the activity is ascribed to Cr(III), possibly with a minor contribution from Cr(II). [11, 13–17] Below monolayer coverage, on alumina, silica and zirconia, a linear relationship has been found between the number of mononuclear Cr(V) and Cr(VI) species after calcination, and catalytic activity after reduction to Cr(III). [11, 18–21]. A candidate for the active species is thus *redox Cr(III)*, described as Cr(III) species resulting from the reduction of high valent chromium. [11, 14, 16, 19, 22–24]. Moreover, mononuclear redox Cr(III) species have been proposed active on the basis of the observed linear increase in activity with chromium loading below 2 wt%. [1, 11, 14, 19, 20, 24] However, by means of atomic layer epitaxy (ALE), Cr/oxide catalysts with active Cr(III) species have been formed without passing through the high-valent state. [25] These species were described as non-redox Cr(III), and several authors propose such chromium centers to be present on amorphous chromia dispersed on the oxide support. [15, 21, 25–27] It thus appears that two types of surface species may be active in catalytic dehydrogenation on Cr/oxide catalysts, or, alternatively, that the activity of a Cr(III) ion is determined by its environment rather than redox history. [25] This view is corroborated by Cavani *et al.* [15] who summarized the topical literature on the subject by stating that activity generally appears to be a function of chromium coverage rather than the initial state of the catalyst.

One approach to exploring the local environment of active Cr(III) is to start out with the surface in a well characterized state and to monitor it during reaction steps leading to the active catalyst. An interesting experiment along these lines was performed by DeRossi *et al.* [11] to clarify the role of oxidation states +II and +III. Using a Cr/silica catalyst with 0.5 wt% chromium, they first calcined the sample and then exposed it to carbon monoxide, thus predominantly reducing chromium to oxidation state +II. The reduced sample was either submitted directly to dehydrogenation, or pre-heated with water to oxidize Cr(II) selectively to Cr(III) before submitting to dehydrogenation. The catalyst was still active after the water treatment, thus proving that Cr(III) is active for dehydrogenation. The water treatment did reduce the activity, though, supposedly due to segregation of chromia to reduce the number of surface chromium centers. Most interestingly, on the basis of IR spectra of CO probe molecules, the authors further proposed that the same active Cr(III) species were formed from Cr(II) under reaction conditions for dehydrogenation as were obtained by oxidation with water. Citing earlier work of Wittgen *et al.* [28], the oxidation under dehydrogenation conditions was ascribed to the reaction of Cr(II) with silanols.

Furthermore, nearly identical IR spectra of CO probe molecules were observed on the water-treated surface as after reduction of the calcined catalyst with H_2. [11] In a separate study, Hakuli *et al.* [13] obtained the same extent of reduction and equal activity after reduction with H_2 as when leaving the calcined catalyst 5 min on stream with i-butane. The Cr(III) species formed through oxidation of Cr(II) with water thus appears to be a candidate for redox Cr(III).

DeRossi *et al.* [11] did not discuss a mechanism for oxidation of Cr(II) to Cr(III), but they did propose a structure for the product Cr(III) species in which chromium is bonded to the surface *via* two oxygen bridges and with hydroxyl as the third ligand. Since they used a low chromium loading of 0.5 wt%, the Cr(III) sites were believed to be mononuclear. In line with this, Jóźwiak *et al.* [29] depicted the reaction of mononuclear Cr(II) to Cr(III) as a reaction with a silanol to give a third Cr–O–Si link to the surface. Recombination of hydrogen atoms produced on separate mononuclear sites would lead to the release of molecular H_2. A similar reaction with water would result in a hydroxyl group on chromium instead of a third Cr–O–Si linkage. However, both of these proposals rely on the release of a hydrogen radical from chromium. Groeneveld *et al.* [9] argued against odd oxidation numbers in the reduction of mononuclear Cr(VI) and pointed out that dinuclear Cr(III) species may be formed from either Cr(II) or Cr(VI) without resorting to odd oxidation states. [9, 30] They also proposed that hydrolysis of Cr(II)–OSi linkages may leave chromium mobile on the silica surface, which would provide a link between mononuclear Cr(II) and polynuclear Cr(III).

In the present work, we use quantum chemistry in conjunction with simple cluster models to examine the proposal by Groeneveld *et al.* [9] that hydrolysis of Cr–OSi linkages would render chromium mobile on the silica surface. We then go on to explore various routes of oxidation to Cr(III) during the encounter of two Cr(II) centers. It is our aim to present reaction energies and activation energies that allow us to consider the feasibility of the proposed schemes and to draw conclusions regarding the nature of potentially active Cr(III) sites on silica.

II. COMPUTATIONAL MODELS

Cluster models of Cr(II)/silica have been constructed in an *ad hoc* manner, drawing on chemical intuition and experimental observations. Three models, presented in Fig. 1, have been constructed for the study of different parts of the reaction between Cr(II)/silica and water. Relatively small clusters have been chosen since this permits the study of reactions, including determination of transition states, for a system which has not previously been studied by theoretical means.

Mononuclear chromium(II) on silica supports has been depicted as anchored *via* two Cr–O–Si linkages. [31, 32] This property is captured in model **A** in Fig. 1, which has been used to study hydrolysis of Cr–OSi linkages. The silica surface is represented by a disiloxyether, the more distant parts of the silica being neglected and dangling bonds terminated with hydrogen. The cluster geometry has been optimized to a minimum on the potential energy surface.

Model **B** in Fig. 1 was made with the purpose to study whether a Cr(II)OH moiety is capable of translation on the surface of amorphous silica. The model was constructed by modification of the *(101)-3bridge* cluster model of Cr(III)/silica which was prepared in Ref. [33]. The structure includes a three-membered SiO ring and a CrOH moiety which coordinates to a surface siloxane of the three-membered ring. The geometry has been relaxed to a minimum on the potential energy surface.

Finally, model **C** in Fig. 1 was constructed with the purpose to study the reaction between two Cr(II)OH moieties. First, an -OCrOCrO- unit was attached to a di-siloxylether molecule and the geometry relaxed within C_S symmetry. Second, the Cr–O–Cr linkage was hydrolyzed to give two -CrOH moieties anchored on vicinal silicon atoms. Keeping the positions of the atoms of the disiloxyether base frozen, the geometry of the -OCrOH moieties was relaxed to a local minimum on the potential energy surface.

Computations with model **B** in Fig. 1 were performed without constraints on geometric parameters. Mimicking restoring forces from the extended silica surface, the atoms of the disiloxyether base in the smaller models **A** and **C** had their positions fixed during reaction studies.

Quantum mechanical (QM) calculations have been performed using density functional theory as implemented in the Amsterdam Density Functional (ADF) set of programs [34–36]. For electron correlation the LDA functional of Vosko *et al.* [37] augmented by the nonlocal 1986 corrections by Perdew [38] was used. The exchange functional consists of the Slater term augmented by gradient corrections as specified by Becke [39]. For details of basis sets and geometry optimization see Ref. [33].

In general, energy differences refer to electronic degrees of freedom only, i. e. without zero-point vibrational energies or temperature effects. In order to take into account temperature and entropy effects, the full set of thermodynamic functions were computed in the harmonic and rigid-rotor approximation for selected structures based on model **C**. Maximal accuracy of the numerical integration schemes was used. All stationary structures display an ultra-soft vibrational mode which consistently has been omitted from the harmonic analysis.

Minimum Energy Crossing Points (MECPs) between spin potential energy surfaces were optimized using ADF, in conjunction with the code developed by Harvey *et al.* [40, 41]. A set of shell scripts and Fortran programs are used to extract energies and gradients for the two spin states and to combine these to produce an effective gradient pointing toward the MECP and used to update the geometry. The convergence criteria are energy differ-

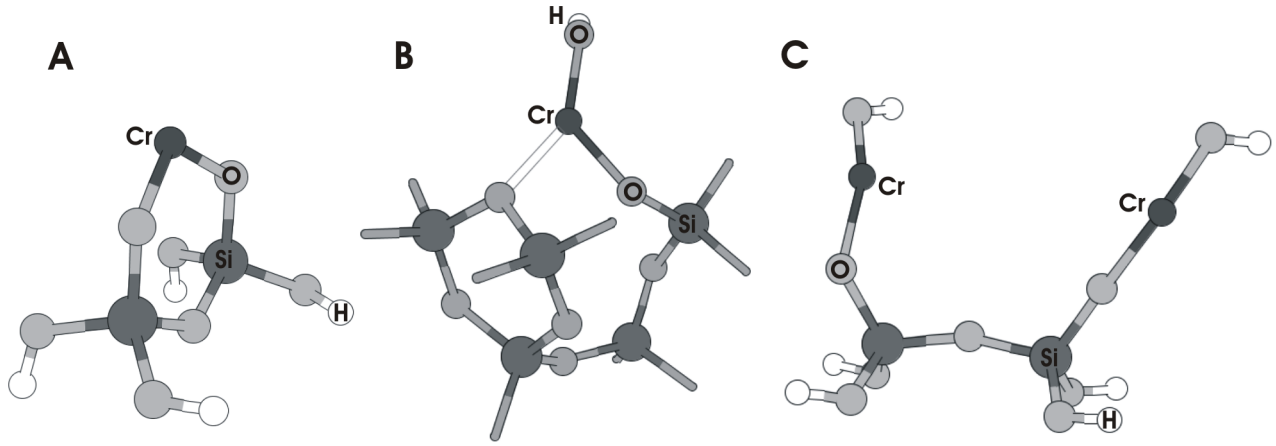

FIG. 1: Models of Cr(II)/silica; mononuclear Cr(II)/silica (**A**), mononuclear Cr(II)OH/silica (**B**), and two mononuclear Cr(II)OH moieties anchored on vicinal silicon atoms on silica (**C**). For the sake of clarity, the terminating SiOH moieties of model **B** are represented by the Si–O bonds only. Polar covalent bonds are indicated by colored sticks, while dative bonds are indicated by blank sticks.

ence less than 0.1 mHartree and an energy gradient, at the seam of crossing, within the normal ADF convergence criterium.

III. RESULTS

We first consider hydrolysis of a Cr–OSi bond in Cr(II) species bonded to an amorphous silica surface through two oxygen linkages. Based on the computed translational barriers it appears that singly-linked Cr(II) centers may be quite mobile, and on this basis we consider several mechanisms of redox reactions in the event of encounters between two Cr(II)OH moieties.

A. Formation and Mobility of Cr(II)OH on the Surface of Amorphous Silica

Cluster $\mathbf{A}_1$ in Fig. 2 represents a Cr(II) site bonded to the silica surface through two oxygen linkages. This site may coordinate one or two molecules of water at an electronic binding energy of about 90 kJ per mole of water. The monohydrated site is shown as structure $\mathbf{A}_1(\mathbf{H}_2\mathbf{O})$ in Fig. 2**a**. There is a low energy barrier of 55 kJ/mol toward hydrolysis of a Cr–O bond to form $\mathbf{A}_2$ in Fig. 2. During this reaction, one hydrogen has been transferred from water to one of the bridging oxygens, to give a silanol moiety, while the remaining hydroxyl part becomes ligated to chromium. At this point, chromium is bonded to the surface *via* a single covalent CrOSi linkage with $rCrO_A$=1.88 Å and a dative bond to the newly formed silanol moiety, with $rCrO_B$=2.21 Å. Rotation of the CrOH moiety away from the coordinating siloxane destroys the dative bond, at an energy cost of 32 kJ/mol. In the structure where the dative bond is broken, cf. $\mathbf{A}_3$ in Fig. 2, the electronic energy is 14 kJ/mol below the reactant asymptote of separated cluster and water molecule.

In the $\mathbf{A}_3$ configuration, the Cr(II)OH moiety is coordinatively highly unsaturated and may coordinate to neighboring oxygen species such as siloxanes or silanols. While the latter is likely to simply reverse the hydrolysis reaction just described, we will see that reaction with a siloxane may constitute a route to transferral of chromium from one silicon tetrahedron to the next one. Stationary structures for such a reaction are presented in Fig. 2**b**. Starting with a CrOH moiety, similar to that in configuration $\mathbf{A}_3$ in Fig. 2, a dative bond may form between chromium and a siloxane in its immediate surroundings. To model this one needs to include a larger section of the silica surface than does the **A** model. Model **B** is obtained by replacing H_B in the $\mathbf{A}_3$ configuration by a six-atom $(SiO)_3$ ring, terminated by hydroxyl groups. One oxygen in the ring coordinates to chromium at a distance of $rCrO_C$=2.23 Å, while the covalent Cr–O bond remains intact at $rCrO_A$=1.88 Å. In the course of the reaction presented in Fig. 2**b**, the CrOH moiety switches from one silicon tetrahedron (Si_A in the figure) to another one (Si_C), and at the same time the six-atom ring in $\mathbf{B}_1$ develops into the larger $(SiO)_4$ ring in $\mathbf{B}_3$.

The first step in this reaction is to coordinate the bridging oxygen of the -O_ACrOH moiety to Si_B of the $(SiO)_3$ ring, cf. $\mathbf{B}_2$ in Fig. 2**b**. Structure $\mathbf{B}_2$ is thus formed in which one silicon, Si_B, is five-coordinated and takes part in both the six-atom ring of structure $\mathbf{B}_1$ and a new eight-atom ring which includes O_A. Relative to $\mathbf{B}_1$, the computed electronic energy of activation is a mere 2 kJ/mol, and the change in energy upon forming $\mathbf{B}_2$ is -18 kJ/mol. At the transition state, the O_A–Si_B distance is 2.56 Å, compared to 2.92 Å and 1.91 Å in the reactant and product structures $\mathbf{B}_1$ and $\mathbf{B}_2$, respectively. An interesting feature of structure $\mathbf{B}_2$ is a four-atom ring composed of Cr, O_A, O_C, and Si_B, cf. Fig. 2**b**, with bond distances $rCrO_A$=2.00 Å, rO_ASi_B=1.91 Å, rSi_BO_C=1.80 Å

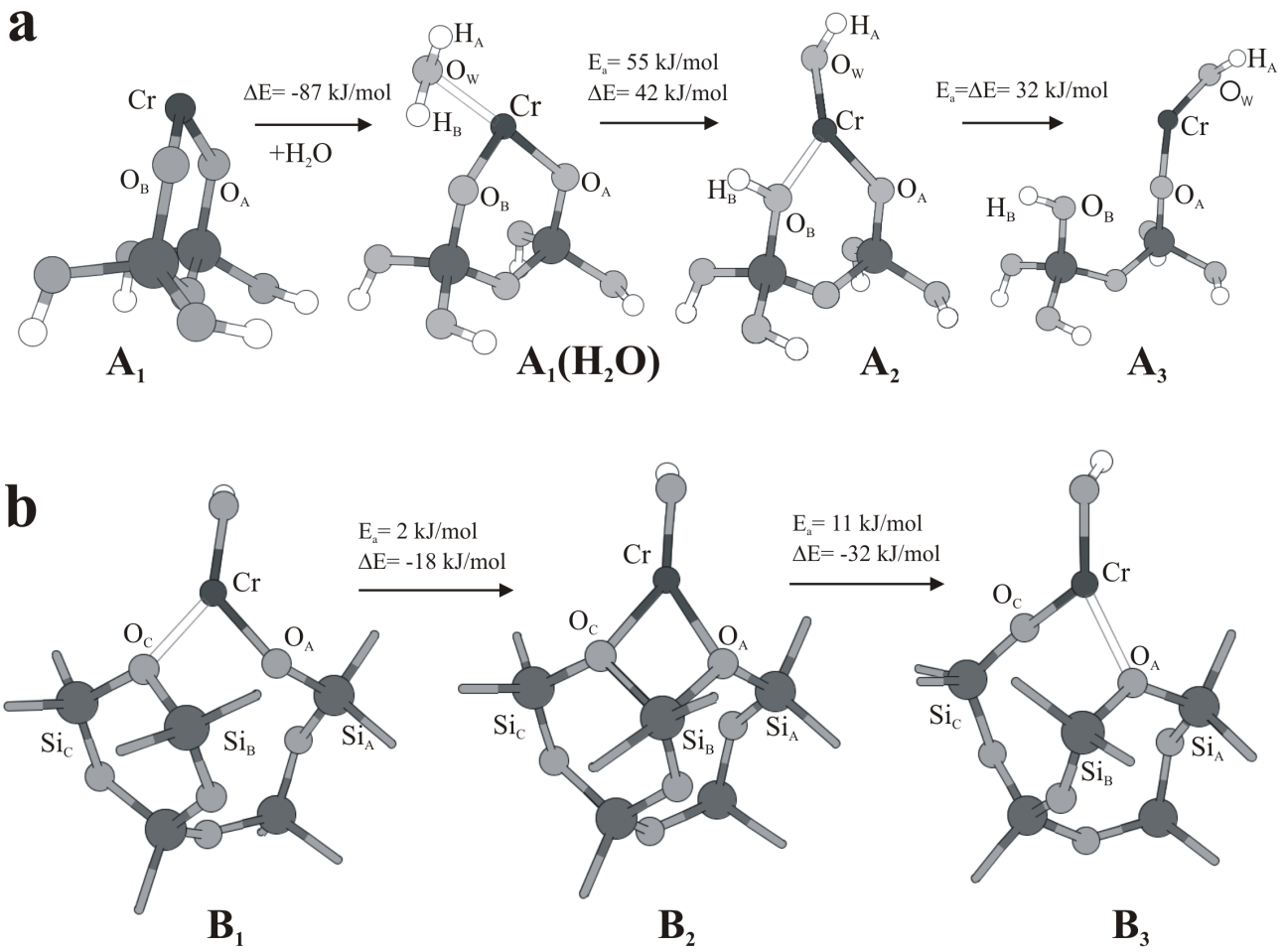

FIG. 2: Optimized stationary structures and electronic energies for the reaction steps leading to relocation of chromium on a silica surface. The main reaction steps are **a**: Hydration of chromium followed by hydrolysis of a Cr–O bond by σ-bond metathesis and rotation of the (-O)CrOH moiety from the silanol group, and **b**: The CrOH moiety traverses from one silicon tetrahedron to another *via* a five-coordinated silicon. For each reaction step in the figure, E_a represents the electronic energy of activation and ΔE is the change in electronic energy.

and rO_CCr=2.06 Å. Although chromium is triply coordinated in the $\mathbf{B}_2$ geometry, the electron spin spin density remains typical for divalent chromium, at 4.1 *e*.

In the final reaction step shown in Fig. 2**b**, the pseudo symmetry of the Cr–O bonds is broken and chromium attains a full covalent bond to O_C while retaining a loose dative bond to a second oxygen, O_A in structure $\mathbf{B}_3$. The Cr–O_C and Cr–O_A bond lengths are 1.92 and 2.24 Å, respectively. This change is of course reflected also in the oxygen-silicon distances, and between structures $\mathbf{B}_2$ and $\mathbf{B}_3$, rO_CSi_B increases from 1.80 to 3.64 Å while rO_ASi_B shortens from 1.91 to 1.71 Å. In the process, a transition state is passed at rO_CSi_B=1.94 Å and rO_ASi_B=1.85 Å, corresponding to an electronic energy of activation of 11 kJ/mol. The change in electronic energy for the reaction is -32 kJ/mol.

Between structures $\mathbf{B}_1$ and $\mathbf{B}_3$, the CrOH moiety has transferred from the Si_A tetrahedron to the Si_C tetrahedron. The overall electronic energy barrier for the reaction is merely 2 kJ/mol and the electronic energy is lowered by 50 kJ/mol. The CrOH moiety may shift further along the silica surface by repeated reactions of the type studied here. In general, the energetic barrier of the reaction will depend on the strain in $(SiO)_n$ rings that are broken and formed, respectively, in addition to constraints imposed by the extended surface which has been ignored in the present computations.

B. Oxidation of Cr(II) to Cr(III)

The previous section described how a Cr(II)OH moiety may migrate on a silica surface. Here, we explore possible redox reactions in the event of a close encounter of two CrOH moieties. Assuming the chromium centers to be separated by two siloxane units, cf. $\mathbf{C}_0$ in Fig 3, they may interact *via* one or two hydroxyls as in structures $\mathbf{C}_2$ and $\mathbf{C}_1$ in the same figure. In either case, hydroxyls that interact with both chromium atoms take on symmetric bridging positions rather than showing a strong and a

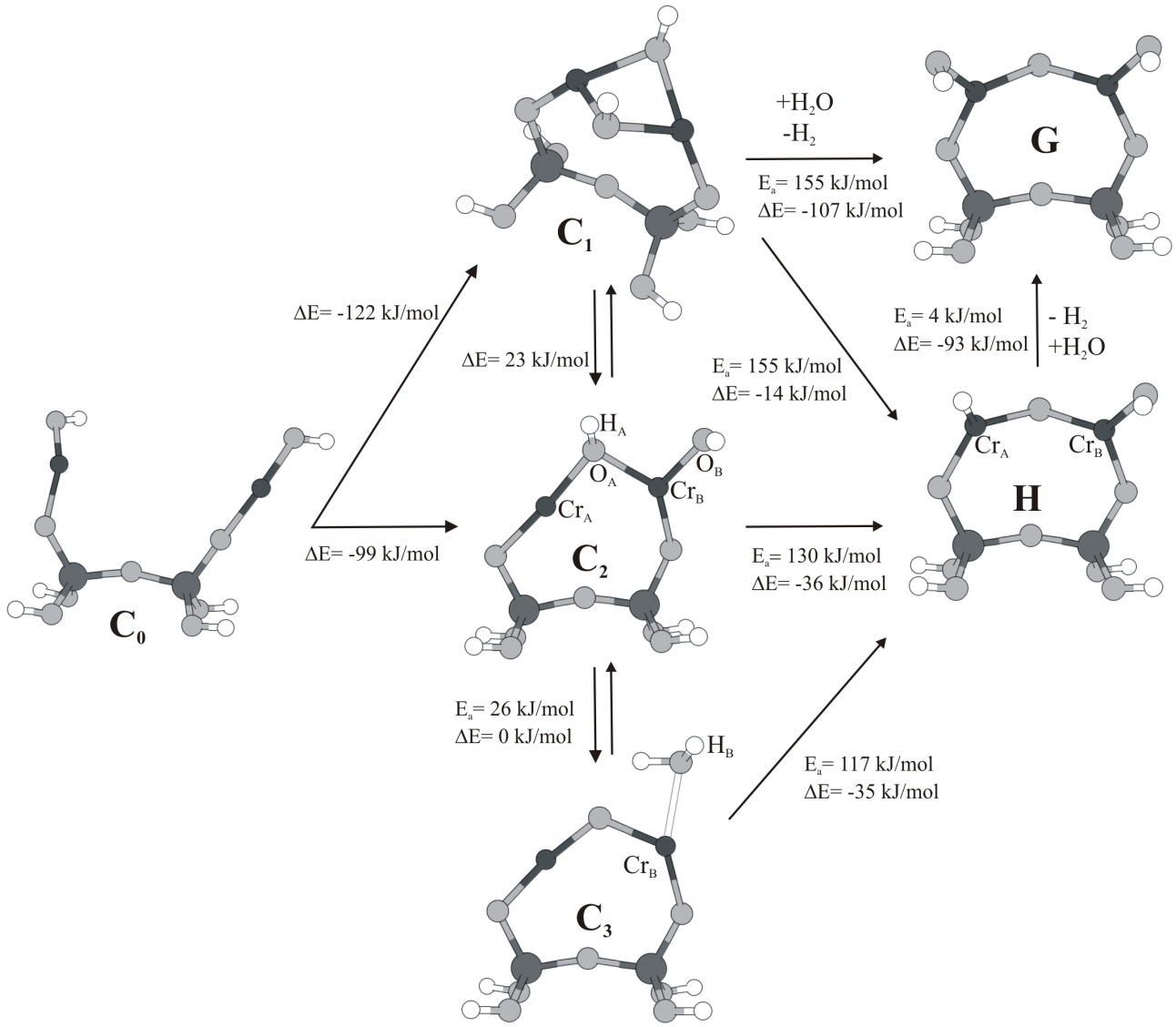

FIG. 3: Optimized stationary structures and electronic energies for the reaction of two CrOH moieties on a silica surface. E_a represents electronic energy of activation, and ΔE is the change in electronic energy. Structures $\mathbf{C}_1$, $\mathbf{C}_2$, and $\mathbf{C}_3$ represent different starting points for oxidation of chromium from II to III, with structures **H** and **G** being the oxidation products. **G** is proposed active for dehydrogenation of alkanes.

weak metal–OH interaction. This may be exemplified by the $\mathbf{C}_1$ structure, which displays a four-membered ring with Cr–OH bond lengths of 2.00 Å, to be compared to Cr–OH bond lengths of 1.82 Å in $\mathbf{C}_0$. This structure was proposed by Wittgen *et al.* [28] as a likely product from the reaction between Cr(II)OCr(II) species and surface silanols. From our computations, the chromium-hydroxyl interactions in $\mathbf{C}_1$ represent a stabilization of 122 kJ/mol relative to the energy of the two separated CrOH moieties in $\mathbf{C}_0$. The electron spin density associated with each chromium atom is 4.1 e in $\mathbf{C}_1$ and 4.2 e in $\mathbf{C}_0$, consistent with divalent chromium in both cases.

The two chromium centers may alternatively share only one hydroxyl group, cf. structure $\mathbf{C}_2$ in Fig. 3, with Cr_A–O_A and O_A–Cr_B distances of 1.99 and 1.94 Å for the bridging OH group, and rCr_BO_B=1.82 Å for the terminal hydroxyl. A difference in electron spin densities develops between the two metal atoms, cf. 4.5 e and 3.6 e on Cr_A and Cr_B, respectively. The $\mathbf{C}_2$ structure is only 23 kJ/mol less stable than $\mathbf{C}_1$, suggesting that they may exist in a dynamic equilibrium.

Structure $\mathbf{C}_2$ in Fig. 3 may rearrange into a μ-oxo dichromium structure in a condensation reaction between the two hydroxyl groups. This leads to structure $\mathbf{C}_3$ where the produced water remains coordinating. The newly formed oxygen bridge is characterized by Cr–O distances of 1.82 and 1.84 Å, where the higher value applies to the chromium holding the coordinated water. Electron spin densities of 4.3 and 4.0 e confirm the divalency of chromium. The electronic energy of activation for the

condensation reaction is only 26 kJ/mol and the reaction is essentially energy neutral, implying that $\mathbf{C}_3$ may be in equilibrium with the two other structures described. Moreover, in agreement with the long H_2O–Cr distance of 2.16 Å, the water in $\mathbf{C}_3$ is fairly weakly bound, by 45 kJ/mol.

In the following, we explore topical reaction paths going from $\mathbf{C}_{1-3}$ to structures **G** and **H** shown to the right in Fig. 3, which constitute oxidation of chromium from +II to +III. Changes in the free energies along the different reaction paths are plotted in Fig. 6.

1. *Oxidation Scheme* **I**

Wittgen *et al.* [28] suggested that hydrogen transfer from a bridging hydroxyl in $\mathbf{C}_1$ to chromium constitutes a viable route from Cr(II) to Cr(III). We have investigated this proposal by means of cluster models as shown at the top of Fig. 4, where H_A is transferred to Cr_B to prepare **D**. We find that in the presence of water, **D** is likely to undergo a series of exothermic steps which include uptake of one molecule of water and release of molecular hydrogen, to make structure **G**. This sequence of events will be described below.

While structures $\mathbf{C}_1$ and **D** in Fig. 4 have almost the same energy, they have different spin states; the former being a nonet while **D** has a septet ground state. This means that the transition state of the reaction $\mathbf{C}_1 \rightarrow \mathbf{D}$ is likely to be found at a Minimum Energy Crossing Point (MECP) between the two potential surfaces. A crossing point is located[40, 41] at an energy of 155 kJ/mol above that of $\mathbf{C}_1$, cf. structure **MECP($\mathbf{C}_1$-D)** in Fig. 4. It is characterized by bond lengths rO_AH_A=1.25 Å, rH_ACr_B=1.77 Å, and rO_ACr_B=1.82 Å. The electron spin density remains close to 4 *e* at Cr_A while that of Cr_B drops to 2.5 *e*. This asymmetry persists to the product, structure **D** in Fig. 4, which displays H_A as a hydrido ligand on Cr_B with rCr_BH_A=1.60 Å. The Cr_A–O_A and O_A–Cr_B bond lengths are 1.90 and 1.71 Å, respectively. This indicates a Cr_A(II)-Cr_B(IV) configuration.

The reaction may proceed from **D** according to Wittgens proposal [28], with the hydrido ligand (H_A) combining with the hydroxyl hydrogen (H_B) to form molecular hydrogen. This leaves a chromium(III) dimer with two chromium and two oxygens forming a four-membered ring, cf. structure **E** in Fig. 4. We have located a transition state connecting **D** and **E** at an energy of 70 kJ/mol above that of the reactant. The reaction step is weakly endothermic. Both the spin density, which is 3.1 *e* at both metal atoms, and the symmetry in the Cr–O distances, which all are 1.82 Å, indicate a Cr(III)-Cr(III) configuration in **E**.

In the presence of water, the reaction does not stop at **E** but rather proceeds by hydrolysis of either of the Cr–O bonds to make the μ-oxo,μ-hydroxo dichromium structure shown as **F** in Fig. 4. The metal–ligand distances are 1.86 and 1.73 Å for the oxo bridge and 2.06 and 1.95 Å for the hydroxo bridge, with values pertaining to Cr_A listed before those of Cr_B. Both bridging ligands are thus closer to Cr_B, which, moreover, holds the terminal hydroxyl. Spin densities of 3.9 and 2.3 *e* on Cr_A and Cr_B confirm a II-IV configuration.

An alternative path from structure **D** to **F** appears by reversing the order of coordination of water and release of H_2. Coordination of water at the hydridochromium center (Cr_B) in **D** is exothermic by 42 kJ/mol. Moreover, the electronic activation energy for hydrolysis of the Cr–H bond followed by elimination of H_2 is almost identical to that of the competing reaction **D**→**E**. Still, the accumulated entropy loss associated with water coordination and the transition state for H_2 formation makes the maximum in free energy some 35 kJ/mol higher for this alternative route to **F**.

From **F**, rotation of the bridging hydroxyl, O_BH_C, shifts this ligand into a terminal position on Cr_A to give structure **G** in Fig. 3 which has two Cr(III)OH centers connected by a covalent oxygen bridge with Cr–O bond lengths of 1.79 Å. The electronic energy of activation for this final step is 28 kJ/mol, and the energy of reaction is -28 kJ/mol. The spin density localized on each chromium center is 3.2 *e*.

Going back to Fig. 3, a competing route to **G** is found by rotation of the bridging hydroxyl in **D** to make the oxo-bridged dichromium site shown as structure **H** in Fig. 5. This step is in fact analogous to the reaction from **F** to **G** and is equally facile with an electronic energy barrier of 25 kJ/mol. The reaction that converts **H** into **G** is discussed in the next subsection.

The free energy profiles of the three reaction paths from $\mathbf{C}_1$ to **G** are plotted in blue lines in Fig. 6. Clearly, the initial oxidation step $\mathbf{C}_1$→**D** is rate determining and it is interesting to note that at the MECP, the free energy is only 33 kJ/mol above that of two separated CrOH moieties given as $\mathbf{C}_0$. After passing the MECP, the routes over **D**→**E**→**F**→**G** (filled squares) and **D**→**H**→**G** (filleds diamonds) appear equally accessible. As mentioned above, there is an alternative path from **D** to **F** which requires significantly higher free energy (filled circles) and thus is rendered unimportant. The reaction free energy from $\mathbf{C}_0$ to **G** is -216 kJ/mol, hence overall the reaction is strongly exothermic.

2. *Oxidation Scheme* **II**

Analogous to the hydrogen transfer reaction described for $\mathbf{C}_1 \rightarrow \mathbf{D}$, a hydrogen may be transferred from the bridging hydroxyl to Cr_A in the singly bridged structure $\mathbf{C}_2$ Fig. 3. This is a two-state reaction involving crossover from the nonet potential surface of $\mathbf{C}_2$ to the septet potential surface. The resulting structure is shown as **H** in Fig. 3. The highest point on the reaction energy profile is found at the Minimum Energy Crossing Point (MECP) between the two potential energy surfaces, at an electronic energy of 130 kJ/mol above that

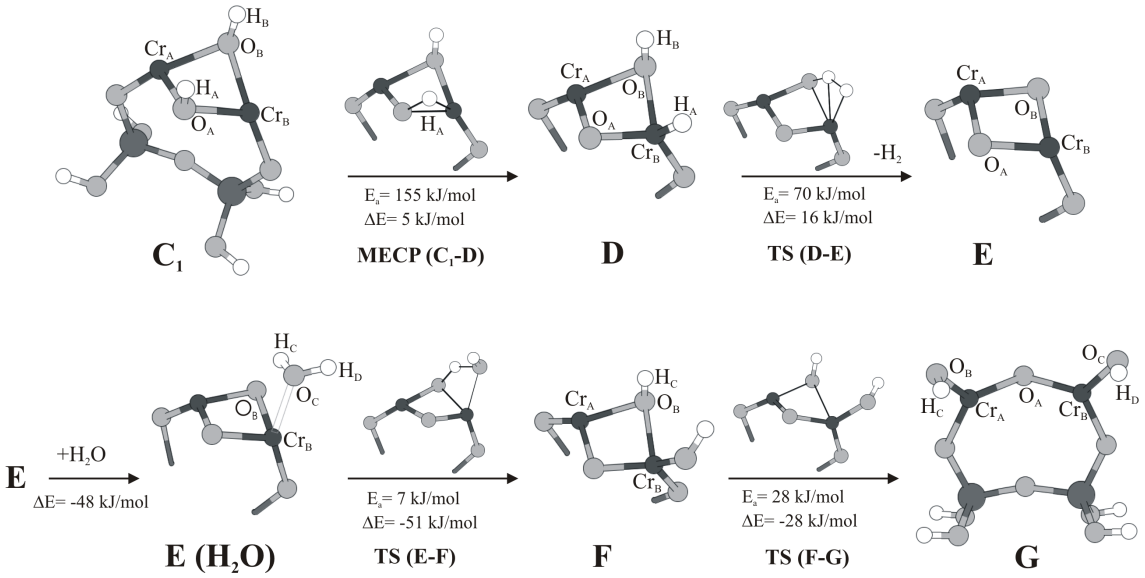

FIG. 4: Optimized stationary structures for the oxidation of Cr(II) to Cr(III) starting from the dimeric chromium structure $\mathbf{C}_1$ in Fig. 3. In order to highlight the reaction, the clusters have been drawn with different degree of truncation of the disiloxyether fragment used to represents the silica surface. E_a denotes the electronic energy of activation, and ΔE is the change in electronic energy.

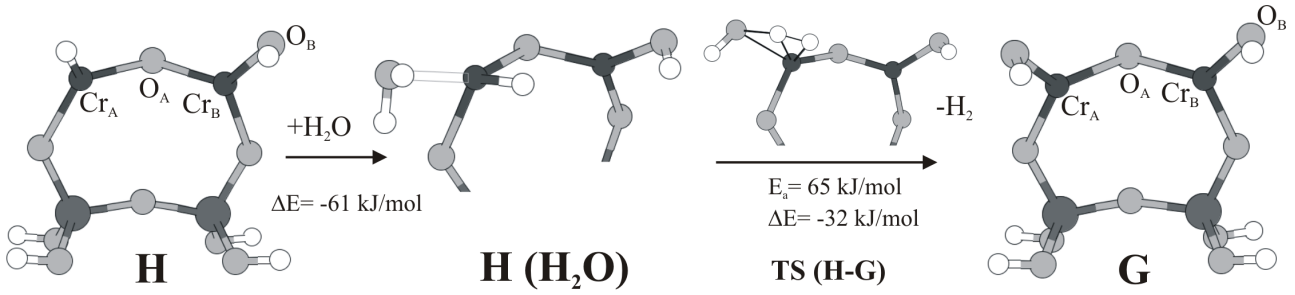

FIG. 5: Optimized structures and changes in electronic energies for the reaction with water of the Cr(III)-hydride center of structure **H**. The reaction results in the formation structure **G** with a hydroxyl on the chromium center, and loss of molecular H_2 to the gas phase. E_a represents the electronic energy of activation, and ΔE is the change in electronic energy for the respective elementary reactions.

of $\mathbf{C}_2$. At the MECP, the Cr_A–O_A–Cr_B distances are 1.90 Å and 1.81 Å, respectively, while rCr_AH_A=1.75 Å, and rO_AH_A=1.31 Å. The spin localized on Cr_A drops by almost a unit, from 4.4 to 3.5 e, while that on Cr_B remains in excess of 3 e. The electronic energy of reaction of -36 kJ/mol. In **H** the Cr_A–O_A–Cr_A distances have now become almost symmetric, at 1.78 and 1.79 Å, and spin densities of 3.3 and 3.2 e on Cr_A and Cr_B show that formal oxidation to Cr(III) has taken place.

The Cr_A–H_A distance in **H** is 1.61 Å, consistent with a polar covalent chromium-hydrogen bond. In the presence of water, this bond is highly susceptible to hydrolysis, a reaction which amounts to exchanging the hydrido ligand for hydroxyl, thus forming **G** in Fig. 3, accompanied by release of H_2. This is illustrated in Fig. fig:reactionHG Relative to the energy of the hydrated complex, the energy of activation for hydrolysis of the Cr–H bond is 65 kJ/mol. and the overall change in electronic energy for the reaction is -93 kJ/mol, cf. Fig. 5.

The free energy profile of the reaction steps from $\mathbf{C}_2$ to **H** is plotted in green (open triangles) in Fig. 6. The oxidation step $\mathbf{C}_2 \rightarrow \mathbf{H}$, i. e. transfer of hydrogen from the bridging hydroxyl to Cr_A, appears to be rate determining for the reaction, with the energy of the MECP some 31 kJ/mol higher than that of the reference structure $\mathbf{C}_0$. This is nearly the same free energy barrier as previously obtained for the oxidation reaction starting out form $\mathbf{C}_1$. After passing the MECP, the hydrolysis at **H** is a secondary bottleneck of the reaction. This also corresponds to the reaction path from $\mathbf{C}_1$. It thus appears that it is equally easy to oxidize two Cr(II)OH centers that interact through one or two bridging hydroxyl ligands.

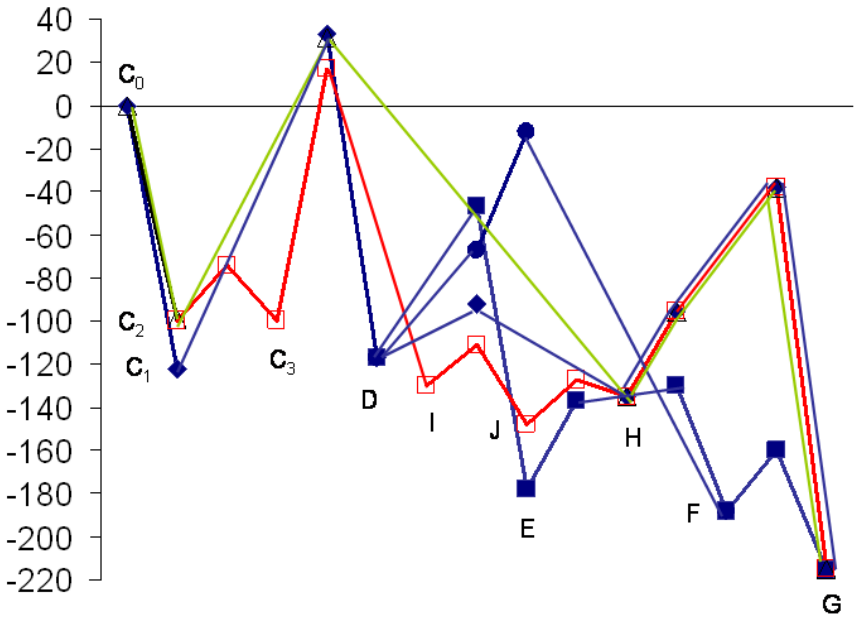

FIG. 6: Free energy plot (kJ/mol) for the oxidation of chromium from +II to +III starting from structure $\mathbf{C}_0$, which is also chosen as the point of zero energy. For reaction steps that only involve rearrangement of bonds in surface species, free energy changes are approximated by electronic energies. For reaction steps that involve adsorption of water or desorption of H_2, free energy changes have been computed explicitly. The reaction paths involving each of $\mathbf{C}_1$, $\mathbf{C}_2$, and $\mathbf{C}_3$ are plotted in blue, green, and red, respectively. The position of stationary structures on the reaction paths through $\mathbf{C}_2$ and $\mathbf{C}_3$ are marked by open black triangles and open red squares, respectively. The reaction path from $\mathbf{C}_1$ splits at **D** into three different paths towards the final product **G**. The path through **E** is marked by filled squares, while the **D**→ **H** path is marked by filled diamonds, and the less accessible alternative path is marked by filled circles.

3. *Oxidation scheme* **III**

Returning to Fig. 3, we have explored a third route to **H** which involves oxidative addition of the coordinated water in structure $\mathbf{C}_3$, followed by migration of a hydrido ligand from on chromium atom to the other. The reactant $\mathbf{C}_3$ Fig. 3, is in a nonet state, with electron spin densities of 4.3 and 4.0 e at the metal centers. Insertion of Cr_B into the O–H_B bond of the coordinated water implies a change to a septet spin state, and a minimum energy crossing point is located at the seam of the two potential energy surfaces. This reaction is illustrated in Fig. 7. Marginally past this MECP, on the septet energy surface, a proper transition state (TS) is located on the septet surface. The electronic energies are nearly the same at the MECP and TS, 117 kJ/mol above the energy of reactant $\mathbf{C}_3$. The length of the activated O_B–H_B bond increases from 0.98 Å in the coordinated water molecule to 1.05 and 1.22 Å at the MECP and TS, respectively. Past the TS, the O_B–H_B bond continues to dissociate and the energy drops to 30 kJ/mol below the energy of structure $\mathbf{C}_3$. The primary product has a divalent spectator chromium (Cr_A), and a four-coordinated chromium (Cr_B), which holds a hydrido and a hydroxyl ligand in addition to two oxygen bridges. The spin density localized on Cr_B drops from 3.7 e in the reactant, to 2.1 e past the MECP. Cr_B is thus formally oxidized from Cr(II) to Cr(IV), while Cr_A remains divalent throughout this reaction step.

The primary product, structure **I** in Fig. 7, has essentially the same electronic energy as structure **H** in Fig. 3 and differs from the latter only in terms of which chromium is holding the hydrido ligand. Not surprisingly, we find that the two structures can be transformed into oneanother *via* a couple of elementary reaction steps with activation energies of ca 20 kJ/mol. Transfer of the hydrido ligand passes over an intermediate structure, **J** in Fig. 7, in which the hydrogen acts as a bridging ligand between the two metal atoms.

Relative to **I**, there is only a small energy barrier of 19 kJ/mol against forming the μ-H structure **J**, and the change in electronic energy is -18 kJ/mol. The electron spin density localized on Cr_A and Cr_B changes from 4.2 and 2.1 e, respectively, in the reactant, to 3.8 and 2.5 e in the hydrogen-bridged structure. In a subsequent step, the hydride may transfer all the way to Cr_A, thus forming structure **H** in Fig. 7 with a Cr_A–H_B distance of 1.61 Å. The electronic energy of activation is 21 kJ/mol and the change in energy of the last step is positive by 13 kJ/mol. Furthermore, as described above, under moist conditions, structure **H** is highly reactive with respect to hydration

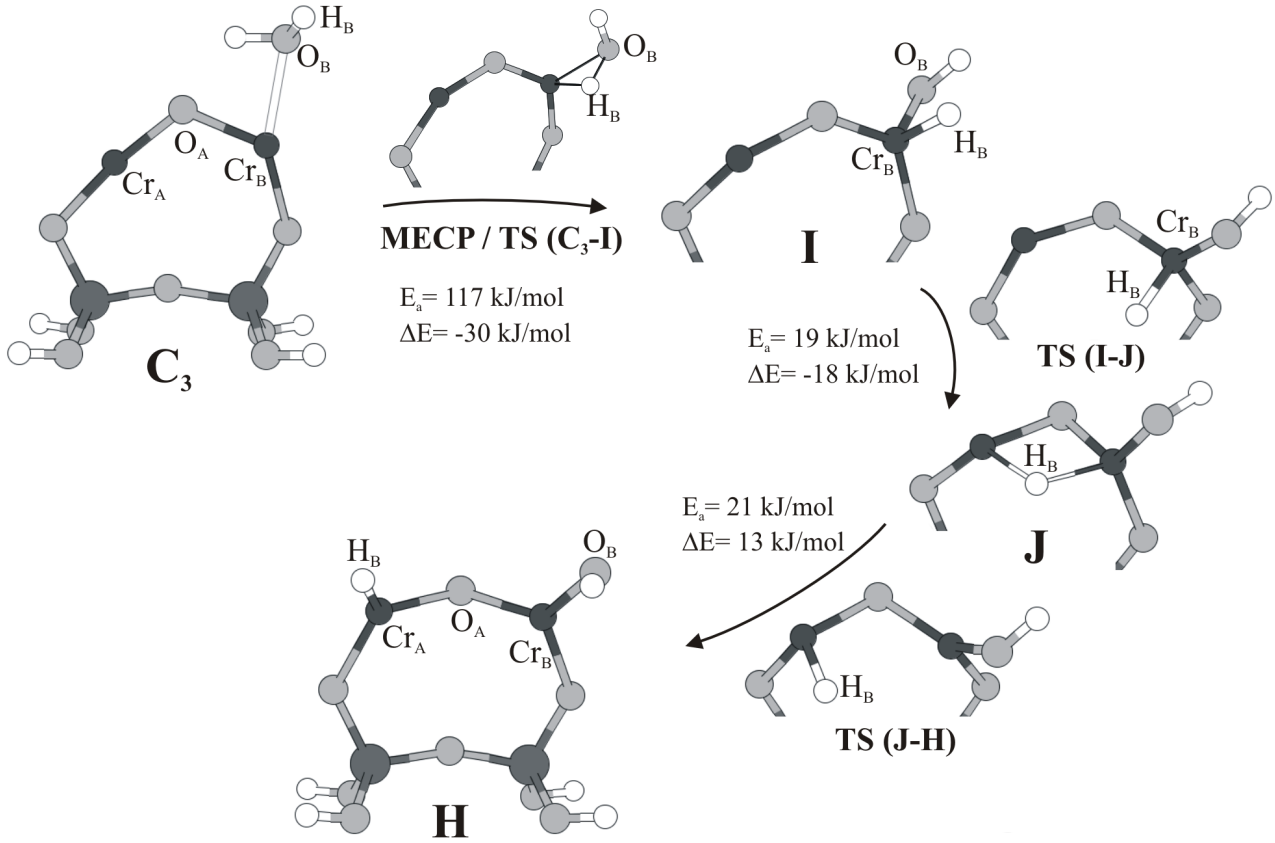

FIG. 7: Optimized structures and electronic energies for the oxidation of the chromium centers in structure $\mathbf{C}_3$. For each reaction step in the figure, E_a represents the electronic energy of activation, and ΔE is the change in electronic energy.

and with respect to hydrolysis to give structure **G**.

The free energy profile of the reaction steps from $\mathbf{C}_3$ to **H** is plotted in red (open squares) in Fig. 6. According to the plot, oxidative addition of water appears to be rate determining. The activation energy relative to $\mathbf{C}_0$ is 17 kJ/mol, which is slightly less than found for oxidation of structures $\mathbf{C}_1$ and $\mathbf{C}_2$ (33 and 31 kJ/mol). Given the limitation in the present models, the difference may be insignificant. The important common feature is that oxidation of Cr(II) to Cr(III) takes place with low barriers for all the three configurations investigated for two interacting Cr(II)OH centers.

In fact, the oxidation steps appear rate determining in all the oxidation schemes studied, cf. Fig. 6. The computed electronic energies of activation relative to structure $\mathbf{C}_0$ are 33, 31, and 17 kJ/mol for oxidation schemes **I**, **II**, and **III**, respectively, all reaction paths leading to the same product structure **G**.

IV. DISCUSSION

We have presented theoretical models of reaction paths for the oxidation of Cr(II) to Cr(III) on amorphous silica, using water as oxidizing agent. Moreover, based on the computations in Ref. [42], the Cr(III) species that is formed appears capable of catalyzing dehydrogenation of ethane with a low activation energy of 91 kJ/mol. [42] These results are in agreement with experimental observations reported by DeRossi *et al.* [11]. There are, however, also some novel implications. As outlined in the introduction, one and the same active species, known as redox Cr(III), may be formed either by oxidation of Cr(II) with water, or by reduction of Cr(VI) and Cr(V) on the calcined surface of Cr/silica. Our results support the idea that the product from oxidation of Cr(II) with water is oligomeric and possibly polymeric. In effect, this indicates that redox Cr(III) species may be of nuclearity higher than one. This is contrary to earlier work, in which redox Cr(III) has been associated with mononuclear species formed at low chromium load. [1, 11, 14, 19, 20, 24]

Recent investigation of Cr/silica by Raman spectroscopy as well as review of literature data led Groppo *et al.* [32, 43] to propose that mononuclear Cr(VI) is the dominant species on surfaces of calcined Cr/silica with chromium load below 2 wt%. Furthermore, the nuclearity appears to be conserved in the subsequent reduction by CO to give Cr(II). [7] However, the situation is more complex for the reduction to Cr(III). Using H_2 as reducing agent, different groups obtained either mainly Cr(II) [12, 13] or mainly Cr(III) [11, 44–46] on Cr/silica

catalysts with chromium load around 1 wt%. These divergent results may be understood in light of observations by Groeneveld *et al.* [9] on the background of the present results. Groeneveld *et al.* [9] found that a high heating rate caused the release of too much water to allow instantaneous removal by the gas flow, and water thus took part in the oxidation of Cr(II) through clustering of Cr(III) oxide. [9] As outlined in the introduction, the authors further proposed that mononuclear chromium(II) might become mobile on the surface of silica by hydrolysis of Cr(II)OSi linkages. [9] Moreover, reaction steps $\mathbf{C_1}$-**D**-**E** of oxidation scheme I in Fig. 4 were proposed for the oxidation of dinuclear Cr(II). Assuming that reduction of mononuclear Cr(VI) by H_2 gives mononuclear Cr(II) and water, the present results suggest that the water may subsequently facilitate the formation of dimers and higher oligomers of Cr(III), the degree of aggregation depending on the partial pressure and residence time of water. Consequently, we propose that in the presence of small amounts of water, redox Cr(III) may form through aggregation and oxidation of chromium(II). In support of this idea, Liotta *et al.* [46] observed gradual aggregation of Cr(III) oxide through cycles of calcination and reduction by H_2. Furthermore, Hakuli et al. [13] reported an increase in the Cr(III)/Cr(II) ratio on H_2-reduced Cr/silica catalysts with increasing chromium load. This is consistent with direct reduction of Cr(VI) to Cr(III) on sites of polynuclear chromates.

Although polymerization appears a viable route to oxidation state +III, our finds do not exclude the formation of mononuclear Cr(III). Reduction of mononuclear Cr(VI) by CO is known to produce mononuclear Cr(II). [7] These sites are oxidized to Cr(III) in the initial contact with alkanes, and it is conceivable that the nuclearity is conserved in this reaction. Mononuclear Cr(III) might also form according to the proposal by Jóźwiak *et al.* [29] as described in the introduction. However, this proposal involves abstraction of a hydrogen radical from chromium and is likely to be associated with a high activation energy. For comparison, our calculations give the total activation energy for dimerization of Cr(II) and subsequent oxidation to Cr(III) of the order of 50 kJ/mol, a number which admittedly carries some uncertainty associated with the specific siloxane structures involved in the translation of Cr(II) on silica as well as the limited size of the present cluster models. It is possible that mononuclear Cr(III) forms subsequent to dimerization, and Wittgen *et al.* [28] suggested that species of dinuclear Cr(III) may react with silanols to form mononuclear doubly anchored Cr(III)OH species. However, when it comes to catalytic activity, the same mechanism of dehydrogenation, with activation energy on the order of 100 kJ/mol, is reported in Ref. [42] for both mono- and dinuclear chromium(III) on silica. The important feature of the active species appeared to be that anchoring to the surface should involve only two ester linkages.

According to the present results, two-bridge chromium(III) centers appear as candidates for the much discussed redox Cr(III) species. Furthermore, the present results and experimental observations [9, 13, 46] have the combined implication that redox Cr(III) may form by oxidation of pairs of Cr(II) centers or possibly through surface reduction of clustered chromium oxide. Noting that *non-redox* Cr(III) is often associated with clustered Cr(III) oxide, [13, 15, 21, 25–27] classification of active Cr(III) on the basis of its redox history may possibly not correspond to actual structures differences at the active centers.

V. CONCLUSIONS

Oxidation of chromium(II) to chromium(III) on the surface of amorphous silica using water as oxidizing agent, has been investigated by means of cluster models and density functional theory. The chromium(III)/silica species resulting from this reaction was reported by DeRossi *et al.* [11] to be active in catalytic dehydrogenation. Furthermore, the species appears as candidate for the much discussed redox Cr(III). The present computations has revealed a viable reaction path that involves dimerization of chromium(II) prior to the oxidation step itself. This in line with a proposal by Groeneveld *et al.* [9] that hydrolysis of Cr(II)–OSi bonds leaves mononuclear chromium(II) mobile on the silica surface. It appears that Cr(II)OH moieties may skip from one silicon tetrahedron to the next by a mechanism that involves changing the pattern of siloxane rings along the path of chromium. The diffusion barrier associated with Cr(II)OH mobility depends on the structural strain of the siloxane rings that are involved in each jump. Oxidation to chromium(III) during the encounter between two Cr(II)OH moieties is found to be facile, and in the presence of moisture, a μ-oxo-bis[Cr(III)OH] species is obtained. Furthermore, computations presented in Ref. [42] indicate that the product species from the oxidation reaction is capable of catalyzing dehydrogenation of ethane with a low barrier. This opens for the possibility that the structural properties of redox Cr(III) are those of higher nuclearity than one even at low chromium load.

[1] Weckhuysen, B. M. and Schoonheydt, R. A. *Catal. Today* **51**, 223 (1999).
[2] Weckhuysen, B. M. and Schoonheydt, R. A. *Catal. Today* **51**, 215 (1999).
[3] Frey, F. E. and Huppke, W. F. *Ind. Eng. Chem.* **25**, 54 (1933).
[4] Weckhuysen, B. M., Wachs, I. E., and Schoonheydt, R. A. *Chem. Rev.* **96**, 3327 (1996).
[5] Kim, D. S., Tatibouet, J.-M., and Wachs, I. E. *J. Catal.* **136**, 209 (1992).
[6] Kim, D. S. and Wachs, I. E. *J. Catal.* **142**, 166 (1993).
[7] Weckhuysen, B. M., DeRidder, L. M., and Schoonheydt, R. A. *J. Phys. Chem.* **97**, 4756 (1993).
[8] Weckhuysen, B. M., DeRidder, L. M., Grobet, P. J., and Schoonheydt, R. A. *J. Phys. Chem.* **99**, 320 (1995).
[9] Groeneveld, C., Wittgen, P. P. M. M., Vankersbergen, A. M., Mestrom, P. L. M., Nuijten, C. E., and Schuit, G. C. A. *J. Catal.* **59**, 153 (1979).
[10] Zecchina, A., Garrone, E., Ghiotti, G., Morterra, C., and Borello, E. *J. Phys. Chem.* **79**, 966 (1975).
[11] DeRossi, S., Ferraris, G., Fremiotti, S., Garrone, E., Ghiotti, G., Campa, M. C., and Indovina, V. *J. Catal.* **148**, 36 (1994).
[12] Lugo, H. I. and Lunsford, J. H. *J. Catal.* **91**, 155 (1985).
[13] Hakuli, A., Harlin, M. E., Backman, L. B., and Krause, A. O. I. *J. Catal.* **184**, 349 (1999).
[14] Hakuli, A., Kytökivi, A., Krause, A. O. I., and Suntola, T. *J. Catal.* **161**, 393 (1996).
[15] Cavani, F., Koutyrev, M., Trifirò, F., Bartolini, A., Ghisletti, D., Iezzi, R., Santucci, A., and Piero, G. D. *J. Catal.* **158**, 236 (1996).
[16] Weckhuysen, B. M., Bensalem, A., and Schoonheydt, R. A. *J. Chem. Soc., Faraday Trans.* **94**, 2011 (1998).
[17] Weckhuysen, B. M., Verberckmoes, A. A., Debaere, J., Ooms, K., Langhans, I., and Schoonheydt, R. A. *J. Mol. Catal. A* **151**, 115 (2000).
[18] DeRossi, S., Ferraris, G., Fremiotti, S., Cimino, A., and Indovina, V. *Appl. Catal. A* **81**, 113 (1992).
[19] DeRossi, S., Casaletto, M. P., Ferraris, G., Cimino, A., and Minelli, G. *Appl. Catal. A Gen.* **167**, 257 (1998).
[20] Kytökivi, A., Jacobs, J. P., Hakuli, A., Merilainen, J., and Brongersma, H. H. *J. Catal.* **162**, 190 (1996).
[21] Hakuli, A., Kytökivi, A., and Krause, A. O. I. *Appl. Catal. A Gen.* **190**, 219 (2000).
[22] Masson, J., Bonnier, J. M., Duvigneaud, P. H., and Delmon, B. *J. Chem. Soc., Faraday Trans. I* **73**, 1471 (1977).
[23] Gorriz, O. F., Corberán, V. C., and Fierro, J. L. G. *Ind. Eng. Chem. Res.* **31**, 2670 (1992).
[24] DeRossi, S., Ferraris, G., Fremiotti, S., Indovina, V., and Cimino, A. *Appl. Catal. A Gen.* **106**, 125 (1993).
[25] Puurunen, R. L., Airaksinen, S. M. K., and Krause, A. O. I. *J. Catal.* **213**, 281 (2003).
[26] Airaksinen, S. M. K., Kanervo, J. M., and Krause, A. O. I. *Stud. Surf. Sci. Catal.* **136**, 153 (2001).
[27] Puurunen, R. L. and Weckhuysen, B. M. *J. Catal.* **210**, 418 (2002).
[28] Wittgen, P. P. M. M., Groeneveld, C., Zwaans, P. J. C. J. M., Morgenstern, H. J. B., Vanheughten, A. H., Vanheumen, C. H. M., and Schuit, G. C. A. *J. Catal.* **77**, 360 (1982).
[29] Jóźwiak, W. K., Ignaczak, W., Dominiak, D., and Maniecki, T. P. *Appl. Catal. A Gen.* **258**, 33 (2004).
[30] Groeneveld, C., Wittgen, P. P. M. M., Swinnen, H. P. M., Wernsen, A., and Schuit, G. C. A. *J. Catal.* **83**, 346 (1983).
[31] Kim, C. S. and Woo, S. I. *J. Mol. Catal.* **73**, 249 (1992).
[32] Groppo, E., Lamberti, C., Bordiga, S., Spoto, G., and Zecchina, A. *Chem. Rev.* **105**, 115 (2005).
[33] Lillehaug, S., Børve, K. J., Sierka, M., and Sauer, J. *J. Phys. Org. Chem.* **17**, 990 (2004).
[34] te Velde, G., Bickelhaupt, F., van Gisbergen, S. J. A., Guerra, C. F., Baerends, E. J., Snijders, J. G., and Ziegler, T. *J. Comput. Chem.* **22**, 931 (2001).
[35] Guerra, C. F., Snijders, J. G., te Velde, G., and Baerends, E. J. *Theor. Chem. Acc.* **99**, 391 (1998).
[36] Baerends, E. J., Autschbach, J. A., Bérces, A., Bo, C., Boerrigter, P. M., Cavallo, L., Chong, D. P., Deng, L., Dickson, R. M., Ellis, D. E., Fan, L., Fischer, T. H., Fonseca Guerra, C., van Gisbergen, S. J. A., Groeneveld, J. A., Gritsenko, O. V., Grüning, M., Harris, F. E., van den Hoek, P., Jacobsen, H., van Kessel, G., Kootstra, F., van Lenthe, E., Osinga, V. P., Patchkovskii, S., Philipsen, P. H. T., Post, D., Pye, C. C., Ravenek, W., Ros, P., Schipper, P. R. T., Schreckenbach, G., Snijders, J. G., Sola, M., Swart, M., Swerhone, D., te Velde, G., Vernooijs, P., Versluis, L., Visser, O., van Wezenbeek, E., Wiesenekker, G., Wolff, S. K., Woo, T. K., , and Ziegler, T. *ADF 2002.03 Computer Code*, (2002).
[37] Vosko, S. H., Wilk, L., and Nusair, M. *Can. J. Phys.* **58**, 1200 (1980).
[38] Perdew, J. P. *Phys. Rev. B* **33**, 8822 (1986).
[39] Becke, A. D. *Phys. Rev. A* **38**, 3098 (1988).
[40] Harvey, J. N., Aschi, M., Schwarz, H., and Koch, W. *Theor. Chem. Acc.* **99**, 95 (1998).
[41] Harvey, J. N. and Aschi, M. *Phys. Chem. Chem. Phys.* **1**, 5555 (1999).
[42] Lillehaug, S. and Børve, K. J. *Submitted to Journal of Catalysis* .
[43] Groppo, E., Damin, A., Bonino, F., Bordiga, S., Zecchina, A., and Lamberti, C. *Chem. Mater.* **17**, 2019 (2005).
[44] Ellison, A., Overton, T. L., and Bencze, L. *J. Chem. Soc., Faraday Trans.* **89**, 843 (1993).
[45] Gaspar, A. B., Brito, J. L. F., and Dieguez, L. C. *J. Mol. Catal. A* **203**, 251 (2003).
[46] Liotta, L. F., Venezia, A. M., Panteleo, G., Deganello, G., Gruttadauria, M., and Noto, R. *Catal. Today* **91**, 843 (1993).